 CMES, vol.93, no.2, pp.149-166, 2013

A Novel Meshless Analysis Procedure for Three-dimensional Structural Problems with Complicated Geometry[1]

Wen-Hwa Chen[2,3], Ming-Hsiao Lee[4]

Abstract: A novel meshless analysis procedure is established for practical implementation in dealing with three-dimensional structures with complicated geometry. By this procedure, to describe the surface of structure, the Stereo-lithography (STL) geometry technique is first adopted. Nodes are then generated and paved uniformly in the space over the entire structure analyzed. To decide the node distribution inside the structure, a geometry-related treatment scheme with relevant checking mechanisms is developed. Besides, a simple and direct spatial integration scheme is also proposed. By this integration scheme, integration points are evenly distributed in the structure and can be adjusted easily to meet the required solution accuracy.

Two three-dimensional structural problems with irregular-shaped geometry are solved to demonstrate the advantages and high efficiency of the present novel meshless analysis procedure.

Keywords: Meshless method, complicated geometry, STL (Stereo-lithography) geometry, Integration scheme

1 Introduction

For practical implementation, one of the main disadvantages of the Finite Element Method (FEM) is that it requires an element mesh, which is constructed by nodes and elements. To create the element mesh for analysis, it is usually tedious and time-consuming. Although the three-dimensional automatic mesh generators gradually become mature in many software programs, it is still not popularly adopted by

[1] This paper is in honor of Professor Wen-Hwa Chen, on the occasion of his receiving the ICCES Lifetime Achievement Medal at ICCES13 in Seattle, in May 2013.

[2] Dept. of Power Mech. Engng., National Tsing Hua University, Hsinchu, Taiwan, ROC.

[3] Corresponding Author

[4] National Center for High-performance Computing, NARL, Taiwan, ROC.

the academia and industry since it can only generate tetrahedral elements instead of preferable hexahedral elements and cannot have the flexibility to use different types of elements at a time, such as shell element, beam element, etc., for certain problems if necessary

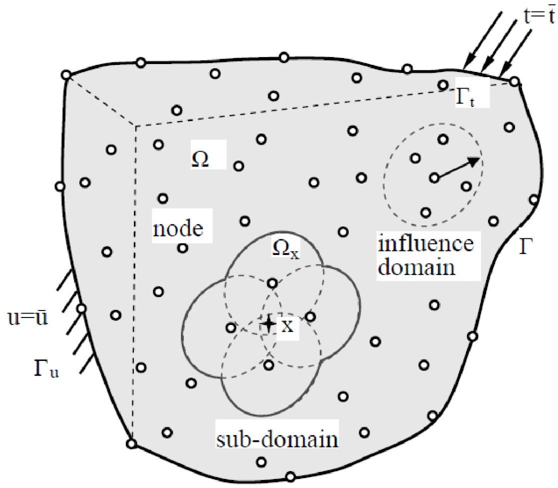

Figure 1: Meshless method

As seen in Fig. 1, the meshless method has an inherent advantage that it doesn't require any elements or element meshes such that it can avoid the shortcomings of the FEM mentioned above. Because of this potential feature, the meshless method has become one of the most promising numerical methods. Based on the similar "meshless" idea, there have been emerging various meshless methods, such as, the element-free Galerkin method (EFGM) (Belytschko et al., 1994), the reproducing kernel particle method (RKPM) (Liu et al., 1995), the h-p clouds method (Duarte and Oden, 1996), and the meshless local Petrov-Galerkin method (MLPG) (Atluri and Zhu, 1998; Cho et al., 1999; Sladek et al. 2013) etc. Although there were pioneering successes by those above methods, most of the cases analyzed were two-dimensional problems in the early works. Till recent years, the three-dimensional problems have then been successfully tackled (Chen and Guo, 2001; Han and Atluri, 2003; Li et al. 2003; Han and Atluri 2004; Chen and Chen, 2005; Lee and Chen 2009; Chen et al., 2009; Chi et al., 2011; etc.) Although the meshless method does not need an element mesh however, it cannot provide sufficient geometric information of the structure as does by the element mesh for the FEM, especially required for the three-dimensional structure with complicated geometry. To solve the difficulties, the STL geometry technique is proposed here. After obtaining the STL-based geometry data, the vertices of the triangular facets (not triangle element) can be taken as the boundary nodes to describe the complicated surfaces of the three-dimensional structure analyzed. To deal with the interior domains or imperfections, a geometry-related treatment scheme with some simple but efficient checking mechanisms are presented.

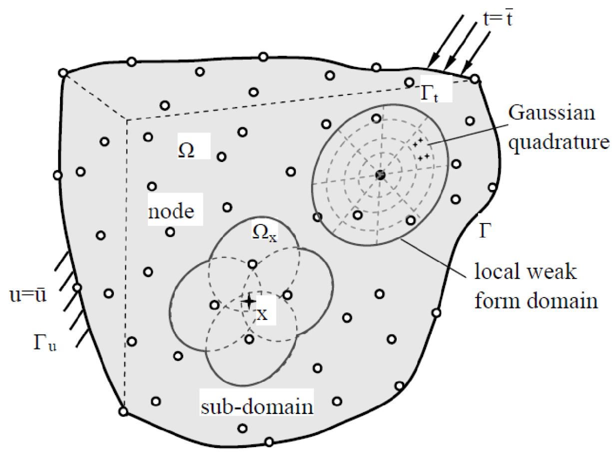

Figure 2: Meshless local Petrov-Galerkin method (MLPG)

As for integrating the integrals of the weak form in the meshless methods, various ways had been devoted. For example, in the MLPG method, an integration sphere which is split into certain amount of sections over which the Gaussian quadrature integration is implemented is used to calculate the local weak form integrals, as shown in Fig. 2. Or, in the EFGM and some other similar meshless methods, the Gaussian quadrature integration is also adopted to obtain the global weak form integrals with a cell structure, as shown in Fig. 3. Although the Gaussian quadrature integration is good for the polynomial interpolation functions as encountered in the FEM, it may induce some deviation of accuracy in the meshless method since its interpolation functions are usually derived by a moving least-squares approximation (Belytschko et al., 1994) and are no longer polynomials. Hence, a uniform integration instead of the Gaussian quadrature integration is proposed herein. Therefore, the integration spheres adopted in the MLPG or the cell structure used by the EFGM are not necessary.

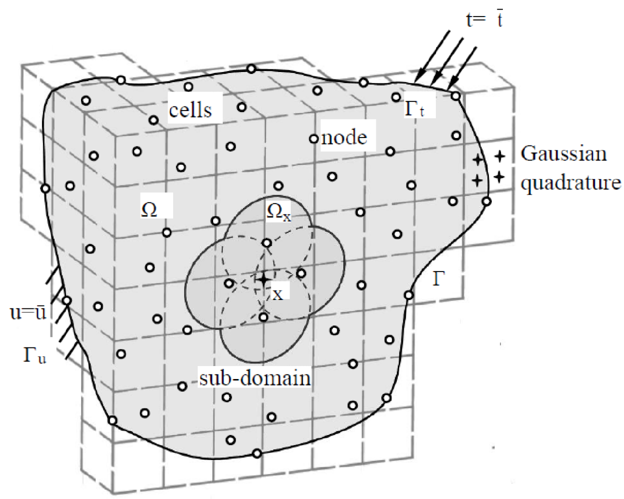

Figure 3: Element free Galerkin method (EFGM)

Consequently, with the mentioned schemes, a novel meshless analysis procedure is thus established to deal with three-dimensional structural problems with complicated geometry. By this procedure, the STL triangulated facets discretized for the analyzed structure, the nodes generated inside the structure and the integration points distributed over the entire structure uniformly can all be performed automatically.

A L3 bone of lumbar vertebrae and an artificial knee joint are then solved as examples by the proposed novel analysis procedure.

2 Formulation for meshless method

The main difference between the FEM and the meshless method is the derivation of the interpolation functions. In the FEM, the element is used to form the interpolation functions which can be used to obtain the field values at certain position inside the element. In the meshless methods, such as MLPG, EFGM and most other meshless methods, no elements can be used to derive the finite- element-like interpolation functions and a moving least-squares approximation is usually adopted to derive the interpolation functions. With those interpolation functions, the formulation for the meshless method can then be proceeded.

2.1 Interpolation functions

As mentioned above, since there isn't any element involved in the meshless method, a moving least-squares approximation is adopted to derive the interpolation functions. As shown in Fig. 1, assume an arbitrary node has an influence domain over certain radius that any point inside the influence domain would be affected by that central node. For a point x, e.g. the integration point, there would be several surrounding nodes within the influence radius and affecting the point x. A combination of the corresponding influence domains of those surrounding nodes determines a sub-domain Ωx. The interpolation functions can then be constructed by implementing the moving least-squares approximation inside the sub-domain (Belytschkoet al., 1994). After this, the field values at any point inside the sub-domain can be calculated through the derived interpolation functions and the field values of the surrounding nodes, as similar to the FEM.

2.2 Basic formulation

To implement the weak form numerically, there are several popular methods employed in meshless methods, such as the collocation method, the Galerkin Method and the Petrov-Galerkin Method (Robert et al, 1974; Huebner and Thornton, 1982)

The collocation method was employed in the smooth particle hydrodynamics (SPH) method for the discretization. The discrete equations of approximation were obtained by enforcing the approximation equation on a set of interior nodes. The equations obtained are just a set of algebraic equations of the unknown variables. This is obviously a simple and fast method, but it has been reported to suffer from instability (Beissel and Belytschko, 1996). The deficiency has been improved by Atluri et al. (2006), with the MLPG method, and much better computing efficiency is achieved.

The Galerkin method as proposed by Belytschko et al. (1994) is a global weak form and has been used to obtain the discrete approximation equations. A quadrature integration based on the cell structure was used to evaluate the integrals. Since the formulation procedure is very similar to that of the FEM, only a basic briefing is described below.

As shown in Fig. 1, consider a general three-dimensional linear elastic isotropic structure Ω, enclosed by its boundary Γ. Based on the principal of minimum total potential energy, the functional Π can be formed as

$$\Pi = \frac{1}{2}\int_{\Omega} \varepsilon^{\mathrm{T}}\mathbf{E}\varepsilon d\Omega - \int_{\Omega} \mathbf{u}^{\mathrm{T}} \cdot \mathbf{b} d\Omega - \int_{\Gamma_t} \mathbf{u}^{\mathrm{T}} \cdot \bar{\mathbf{t}} d\Gamma = \min$$

where ε is the strain, $\mathbf{u}$ is the displacement, $\mathbf{b}$ is the body force, $\bar{\mathbf{t}}$ is the prescribed traction applied at the boundary Γ_t, and $\mathbf{E}$ is the material matrix. The displacement $\mathbf{u}$ at any position of the structure can be interpolated from the global nodal displacement $\mathbf{D}_{3Nx1}$ by the global interpolation function Ψ_{3x3N}

$$\mathbf{u} = \mathbf{\Psi}_{3x3N}\mathbf{D}_{3Nx1} \tag{1}$$

N is the total number of nodes. From the relation between the strain $\boldsymbol{\varepsilon}$ and displacement $\mathbf{u}$, the strain $\boldsymbol{\varepsilon}$ can be derived as

$$\boldsymbol{\varepsilon} = \mathbf{B}_{6x3N}\mathbf{D}_{3Nx1} \tag{2}$$

$\mathbf{B}$ is the gradient matrix for strain $\boldsymbol{\varepsilon}$.

Following a similar derivation procedure for the FEM, the final system of linear algebraic equation can be formed as

$$\mathbf{K}_{3Nx3N}\mathbf{D}_{3Nx1} = \mathbf{F}_{3Nx1} \tag{3}$$

where

$$\mathbf{K}_{3Nx3N} = \int_{\Omega} \mathbf{B}^{\mathrm{T}}\mathbf{E}\mathbf{B}d\Omega$$

and

$$\mathbf{F}_{3Nx1} = \int_{\Omega} \mathbf{\Psi}^{\mathrm{T}}\mathbf{b}d\Omega + \int_{\Gamma_t} \mathbf{\Psi}^{\mathrm{T}}\bar{\mathbf{t}}d\Gamma$$

In the above, $\mathbf{K}_{3Nx3N}$ is the global stiffness matrix and $\mathbf{F}_{3Nx1}$ is the global load vector.

After solving the final system of linear algebraic equation (3), the global nodal displacement $\mathbf{D}_{3Nx1}$ and the field values at any positions of the structure, such as displacement and strain can therefore be computed from eq. (1) and (2) accordingly.

It is noted that each nodal interpolation function is derived from the nodes included in its sub-domain. Hence, how to accurately determine the nodes in the sub-domain is very important.

2.3 Numerical calculation of integrals

The global stiffness matrix $\mathbf{K}_{3Nx3N}$ and global load vector $\mathbf{F}_{3Nx1}$ should be accurately and efficiently calculated over the entire structure analyzed. In general, each entry of the global stiffness matrix $\mathbf{K}_{3Nx3N}$ or global load vector $\mathbf{F}_{3Nx1}$ can be computed as the following integrals

$$\begin{aligned}
&\int\limits_{\Omega} f d\Omega = \sum_{i}^{n_p}\sum_{j}^{n_q}\sum_{k}^{n_l}\alpha_i\beta_j\gamma_k f_{ijk}\\
&\int\limits_{\Gamma_t} g d\Gamma_t = \sum_{i}^{n_r}\sum_{j}^{n_s}\alpha_i\beta_j g_{ij}
\end{aligned} \tag{4}$$

where (f, g) are the functions, (α_i , β_i, γ_i) are the weighting for the *i*th integration point in the *i*-th direction and (n_p, n_q, n_l, n_r, n_s) are the total numbers of integration points taken for integration. Various schemes have been proposed for choosing appropriate integration points and weighting functions.

As mentioned earlier, to obtain the integrals of the weak form in the meshless methods, various ways had been proposed. In the MLPG, only local weak form is adopted (Atluri and Zhu, 1998). As seen in Fig. 2, the local weak form is formed within a sphere surrounding certain nodes and the spatial integration is performed on each independent sphere. The sphere is regularly divided into small segments for numerical integration by Gaussian quadrature integration. In the EFGM, the domain integration for global weak form is needed. The Gaussian quadrature integration over a cell structure is also normally adopted (Fig. 3). In the Gaussian quadrature integration, the integration points selected are not uniformly distributed and weighted, which is good for polynomial type of interpolation functions as encountered in the FEM. It may induce inaccuracy for meshless methods because their interpolation functions derived by the moving least-squares approximation are no longer polynomials. The Gaussian quadrature points are no longer the best ones to sample the interpolation functions and then weighting values. In particular, when the integration volume of certain integration point crosses the surface of the three-dimensional structure, the improper estimations may induce significant inaccuracy. Hence, a uniform integration scheme instead of Gaussian quadrature integration is proposed herein. The uniform integration scheme is also based on the global weak form subject to the principal of minimum total potential energy. By this scheme, every uniformly distributed integration point has same weight in the structure and spatial integration can be performed. In addition, better stability and accuracy are achieved. Furthermore, the density of the integration points can be easily adjusted to meet the required accuracy. Although Beissel and Belytschko (1996) also proposed a direct nodal integration by taking the nodes as integration points, the numerical instability of under-integration due to insufficient number of integration points needs to be overcome.

3 Conventional meshless analysis procedure

Although there are many meshless methods being proposed, their general analysis procedure can be summarized as the follows:

1. Generate the node data for the structure analyzed
2. Select a regular sphere for each node for the MLPG (see Fig. 2) or create the cell structure of which the cells are regularly distributed to cover the entire structure and its boundaries for numerical integration for the EFGM (see Fig. 3)
3. Form the global stiffness matrix $\mathbf{K}_{3Nx3N}$, which includes
   - Integrate the integrals over spheres or cells by Gaussian quadrature.
   - Ignore the quadrature points in spheres or cells outside the structure.
   - Select the sub-domain for each quadrature point inside the structure.
   - Calculate the interpolation function for each quadrature point by the moving least-squares approximation.
   - Assemble the stiffness matrix $\mathbf{K}_{3Nx3N}$ from all the quadrature points.
4. Form the global load vector $\mathbf{F}_{3Nx1}$
5. Solve the equation $\mathrm{K}_{3Nx3N}\mathbf{D}_{3Nx1}$=$\mathbf{F}_{3Nx1}$ to obtain the solution.

However, there are some difficulties encountered in conventional meshless analysis procedure for practical implementation. As for node generation, for two-dimensional or three-dimensional problem with simple geometry, nodes can be generated manually and directly. Even so, unless a very detailed node distribution adopted, the uncertainty for the node distribution sometimes cannot be avoided. For example, as shown in Fig. 4, many different problems are represented by the same one node distribution which is not detailed enough. Besides, in addition to the requirement of the spheres for the MLPG or the cell structure for the EFGM, it is also difficult to determine whether the quadrature points in spheres or cells outside the structure or to exclude the nodes from the sub-domain for the quadrature point accurately since it lacks geometric information. Those above difficulties get more serious especially in dealing with three-dimensional structure with complicated geometry and should be solved.

Some techniques were devoted to the literature. For example, an indirect finite element-like approach is presented (Liu, 2010), where the three-dimensional structure is first discretized in finite elements and then solved by the meshless method. By this method, unfortunately, the merits of the meshless method are sometimes sacrificed

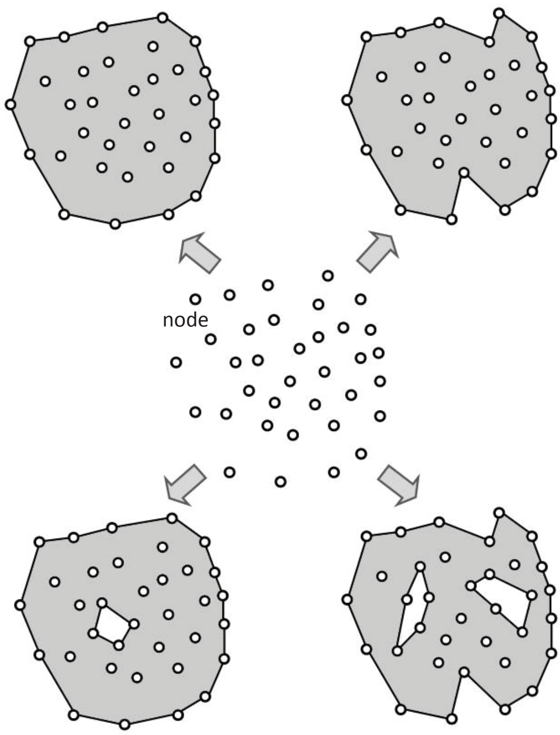

Figure 4: The ambiguity of node distribution in meshless method

4 Present novel meshless analysis procedure

As compared with the conventional meshless analysis procedure, the present novel procedure for the analysis of three-dimensional structure with complicated geometry can be viewed as those following steps:

1. **Establish the STL-based geometry data of the structure analyzed and determine its boundary nodes.** For clarity, as shown in Fig. 5, a L3 bone of the lumbar vertebrae is taken as first example for explanation. Now, the surfaces of the L3 bone can be represented by triangular facets and stored in the STL format as seen in Fig. 6. This can be easily generated by most computer-aided or scanning tools depending on the material characteristics of the object studied. After obtaining the STL-based geometry data, the vertices of the triangular facets can be taken as the boundary nodes for the meshless analysis.

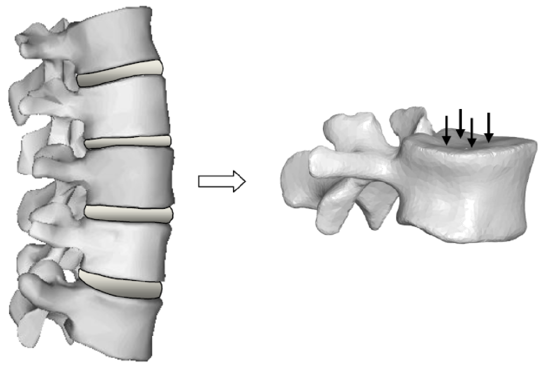

Figure 5: The L3 bone of the lumbar vertebrae

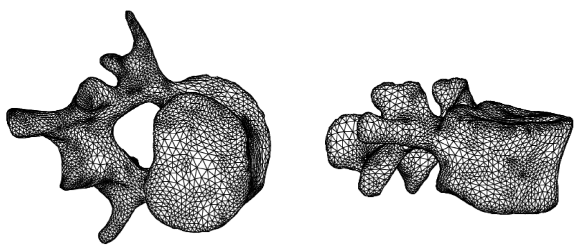

Figure 6: The STL geometry and boundary nodes of the L3 bone

2. **Pave sufficient nodes over entire structure uniformly**, as shown in Fig 7.

3. **Determine the interior nodes of the structure by a geometry-related treatment scheme with relevant checking mechanisms.** How to determine the nodes inside the structure represented by the STL-based geometry is a significant step for the present procedure. As seen in Fig. 8, it explains a geometry checking mechanism for determining if certain nodes are located inside the structure. First of all, one can arbitrarily take a reference point outside the structure. Then, connect the discussed node to the external reference point and check how many times the connecting line crosses the surface of the structure analyzed. When the connecting line crosses the surface an odd number of times, it means that the discussed node lies inside the structure. Otherwise, the discussed node is outside the structure. Other related geometry checking mechanisms can be referred to the work (Lee and Chen,

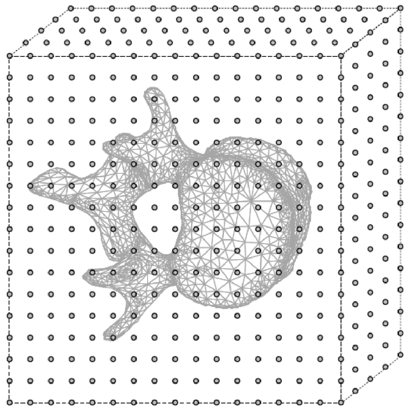

Figure 7: Pave sufficient nodes over the entire L3 bone uniformly

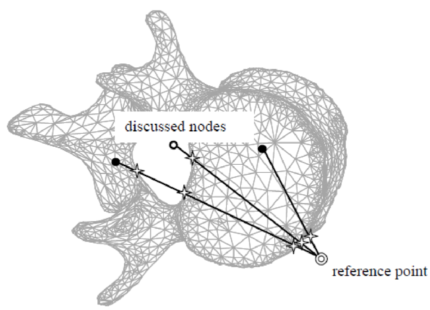

Figure 8: Determine the interior nodes of the L3 bone

2010). Those mechanisms can effectively choose the correct nodes for deriving the interpolation functions even there are internal defects or complicated concave boundaries within the three-dimensional irregular shaped structure. Therefore, by steps(1)-(3), the difficulties encountered for node generation in conventional meshless analysis procedure due to the lack of sufficient geometric information can thus be solved. The final interior nodes for the L3 bone of the lumbar vertebrae are displayed in Fig. 9.

4. **Form the global stiffness matrix $\mathbf{K}_{3Nx3N}$** , which includes

   - **Pave integration points over entire structure uniformly**, as shown in

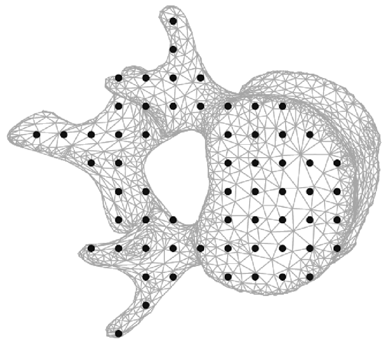

Figure 9: The determined interior nodes of the L3 bone

Fig. 10.

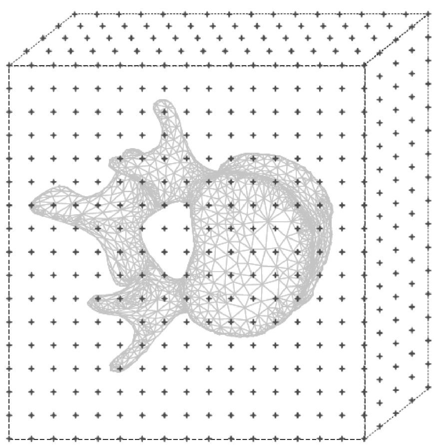

Figure 10: Pave integration points over the entire L3 bone uniformly

- **Exclude the integration points outside the structure or the nodes outside the sub-domain by similar checking mechanisms**. Fig. 11 denotes the screened integration points for the analysis of the L3 bone of the lumbar vertebrae. Fig. 12 displays the choice of nodes in the sub-domain for deriving the interpolation function of an integration point. Once the connecting line between the discussed node and the integration point crosses the surface, the discussed node should be excluded.

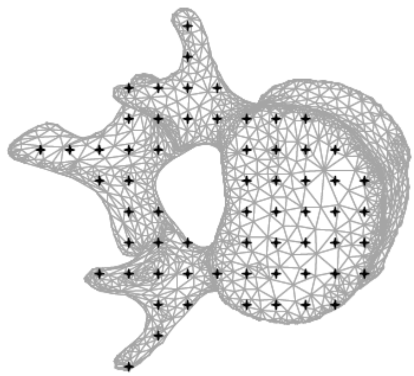

Figure 11: The screened integration points inside the L3 bone

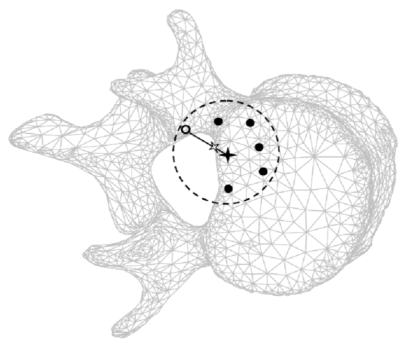

Figure 12: The choice of nodes in the sub-domain of an integration point

- **Integrate the integrals by uniform integration points**
- **Calculate the interpolation functions for the integration points by the moving least-squares approximation**.
- **Assemble the global stiffness matrix $\mathbf{K}_{3Nx3N}$ from all the integration points**

5. **Form the global load vector $\mathbf{F}_{3Nx1}$**
6. **Solve the equation $\mathbf{K}_{3Nx3N}\mathbf{D}_{3Nx1}$=$\mathbf{F}_{3Nx1}$ to obtain the solution**

Since all the operations stated above can be easily programmed and proceeded automatically, by our experiences, the present proposed meshless analysis is very efficient in dealing with three-dimensional structure with complicated geometry.

5 Results and Discussion

To demonstrate the advantages and efficiency of the novel meshless analysis procedure, two biomechanics problems are analyzed. In general, the medical parts, either natural or man-made, are used to fit the human's body and their shapes are usually irregular and complicated. These types of structure always are difficult to solve by conventional meshless analysis procedure. On the contrary, by the present proposed meshless analysis procedure, the works are much more simple and straightforward.

The first example is the analysis of the forementioned L3 bone of the lumbar vertebrae. The spine has five regions: cervical, thoracic, lumbar, sacrum and tail-bone. The lumbar region consists of five vertebrae. Each of them is connected with others by ligaments. The lumbar region provides most support for the upper body and each vertebra is subjected to a vertical normal pressure while standing still. Assume the L3 bone is subjected to a vertical load of 1200 N, approximately two times the weight of a 60 kg person. The Young's modulus of the bone is 100 Mpa, and the Poisson's ratio is 0.2 (Goel et al., 1995). The present computed von-Mises stress distribution of the L3 bone with 2,729 nodes is shown in Fig. 13. The computed displacements and the von-Mises stresses at those representative positions are displayed in Fig. 14 (a) and (b), respectively. Also shown for comparison are the finite element solutions computed by ANSYS software with 19,288 nodes and 11,433 10-node tetrahedral elements. Reasonable agreement between the solutions obtained by the present meshless analysis procedure and ANSYS' can be viewed. As mentioned earlier, it is noted that the present meshless solution can be easily improved by adjusting the density of nodes or integration points if necessary.

Knee replacement surgery replacing the knee joints with artificial parts due to diseased or damaged joint surfaces of knee can well reduce the patient's pain in knees and improve the patient's motion so that it has become a popular treatment for osteoarthritis currently. The quality of the knee replacement requires not only the medical surgery but also the design of the artificial parts which need to fit the patient's unique and complicated bones well in order to maintain good performance. Therefore the structural analysis for the parts is imperative to improve the design to meet the structural requirement. An artificial knee system consists of several parts. The main one is the femur head, normally made of Co-Cr-Mo alloy, as shown in Fig. 15. The femur head is subjected to various loading in different postures. The stiffness of the part is a basic requirement for the part design. Here, a typical loading type is shown in Fig. 15 that one side is fixed and the other side is subjected to a load of 720 N, about the weight of a 70 kg person. The STL-based geometry model obtained by three-dimensional scanning is also shown in Fig. 15. The

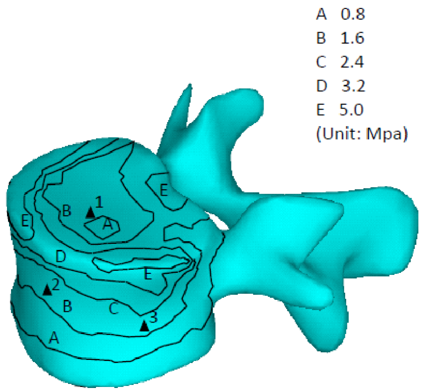

Figure 13: The von-Mises stress distribution of the L3 bone

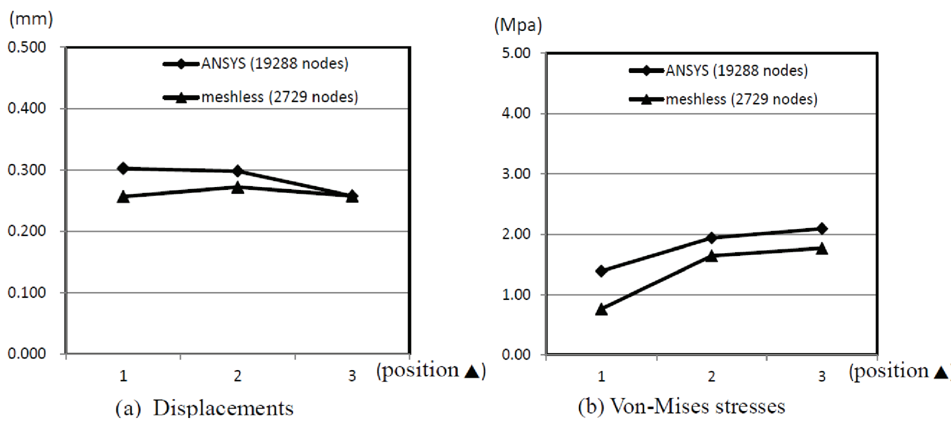

Figure 14: The comparison of the displacements and von-Mises stresses at representative positions

Young's modulus and Poisson's ratio of Co-Cr-Mo alloy are 220,000 Mpa and 0.3 respectively.

The computed displacement distribution in the femur head of the artificial knee system by the present novel meshless analysis procedure with 3,419 nodes is shown in Fig. 16. The comparison of maximum displacement (at point 1) and von-Mises stress (at point 2) with ANSYS program, with 4,383 nodes and 17,940 4-node tetrahedral elements is listed in Table 1. Good agreement between the present meshless analysis and ANSYS' is again found.

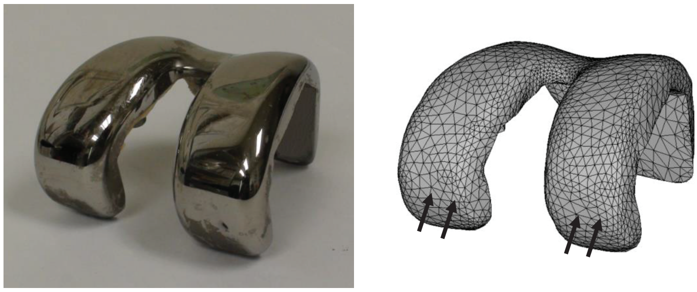

Figure 15: The femur head of the artificial knee system and its STL geometry

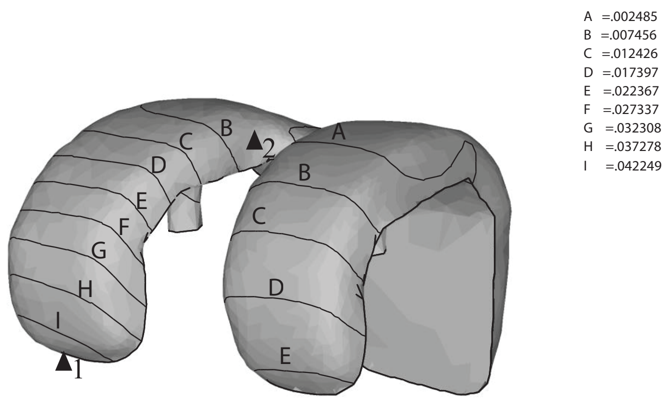

Figure 16: The displacement distribution in the femur head of the artificial knee system

6 Concluding remarks

By the development of STL geometry, geometry-related treatment with relevant checking mechanisms and uniformly paved nodes, sufficient geometric information needed in meshless analysis can be thus provided in the present novel meshless analysis procedure. The difficulties encountered in conventional meshless analysis procedure are therefore avoided even in dealing with three-dimensional structure with complicated geometry. In addition, since the uniform integration scheme instead of Gaussian quadrature integration is adopted, the integration spheres for MLPG or the cell structure for EFGM are no longer required. Besides, the density of the uniformly paved nodes and integration points can be easily adjusted to meet the required solution accuracy if necessary. It is worthwhile to note that all the operations in the present novel meshless analysis procedure can be implemented or

Table 1: The comparison between the computed results by the present meshless analysis and ANSYS program

	Present meshless analysis	ANSYS program
Max. displacement	0.0447 mm	0.0417 mm
Max. von-Mises stress	39.7 Mpa	43.1 Mpa

programmed almost automatically.

The proposed novel meshless analysis procedure can also be easily extended and applied to deal with three-dimensional multi-material or multi-body problems and will be presented in subsequent reports.

References

Atluri, S. N.; Zhu, T. (1998): A new meshless local Petrov-Galerkin (MLPG) approach in computational mechanics. *Comput. Mech.*, vol. 22, pp. 117–127.

Atluri, S.N., Liu, H.T., Han, Z.D. (2006): Meshless local Petrov-Galerkin (MLPG) mixed collocation method for elasticity problems. Computer Modeling in Engineering & Sciences, vol. 14, no. 3, pp. 141-152.

Beissel, S.; Belytschko, T. (1996) : Nodal integration of the element-free Galerkin method. *Comput. Methods Appl. Mech. Engrg.,* vol. 139, pp. 47-49.

Belytschko, T.; Lu, Y.Y.; Gu, L. (1994): Element-Free Galerkin Method. *International Journal for Numerical Methods in Engineering,* vol. 37, pp. 229-256.

Chen, W. H.; Guo, X. M. (2001): Element Free Galerkin Method for Three-dimensional Structural Analysis. *Computer Modeling in Engineering & Sciences,* vol. 2, no. 4, pp. 497-508.

Chen, W. H.; Chen, C. H. (2005): On Three-Dimensional Fracture Mechanics Analysis by an Enriched Meshless Method. *Computer Modeling in Engineering & Sciences,* vol. 8, no. 3, pp. 177-190.

Chen, W. H.; Chi, C. T.; Lee, M. H. (2009): A Novel Element-Free Galerkin Method with Uniform Background Grid for Extremely Deformed Problems. *Computer Modeling in Engineering & Sciences,* vol. 40, no. 2, pp. 175-199.

Chi, C. T.; Lee, M. H.; Chen, W. H. (2011): A Three-dimensional Adaptive Strategy with Uniform Background Grid in Element-free Galerkin Method for Extremely Large Deformation Problems. *Computers, Materials, & Continua,* vol. 24, no. 3, pp. 239-256.

Cho, J.Y.; Kim, H.G.; Atluri, S.N. (1999): A Critical Assessment of the Truly

Meshless Local Petrov Galerkin (MLPG) and Local Boundary Integral Equation (LBIE) Methods. *Computational Mechanics,* vol. 24, no. 5, pp. 348-372.

Duarte, C. A.; Oden, J. T. (1996): An h-p adaptive method using clouds. *Comput. Methods Appl. Mech. Engrg.,* vol. 139, pp.237-262.

Goel, V.K.; Ramirez, S.A.; Kong, W.; Gilbertson, L.G. (1995) : Cancellous Bone Young's Modulus Variation Within the Vertebral Body of a Ligamentous Lumbar Spine—Application of Bone Adaptive Remodeling Concepts. *Journal of Biomechanical Engineering,* vol. 117, pp. 266-271.

Han, Z. D. ; Atluri, S. N. (2003) : Truly Meshless Local Petrov-Galerkin (MLPG) Solutions of Traction & Displacement BIEs. *Computer Modeling in Engineering & Sciences,* vol. 4, no. 6, pp. 665-678.

Han, Z. D.; Atluri, S. N. (2004): Meshless Local Petrov-Galerkin (MLPG) approaches for solving 3D Problems in elasto-statics. *Computer Modeling in Engineering & Sciences,* vol. 6, no. 2, pp. 169-188.

Huebner, K. H.; Thornton, E. A. (1982): The finite element method for engineers, John Wiley & Sons.

Lee, M. H.; Chen, W. H. (2009): A Three-Dimensional Meshless Scheme with Background Grid for Electrostatic-Structural Analysis. *Computers, Materials, & Continua,* vol. 11, no. 1, pp. 59-77.

Lee, M. H.; Chen, W. H. (2010): Geometry related treatments for three-dimensional meshless method. *Computer Modeling in Engineering & Sciences,* vol.61, no.3, pp.249-271.

Li, Q.; Shen, S.; Han, Z. D. ; Atluri, S. N. (2003) : Application of Meshless Local Petrov-Galerkin (MLPG) to Problems with Singularities, and Material Discontinuities, in 3-D Elasticity. *Computer Modeling in Engineering & Sciences,* vol. 4, no. 5, pp. 567-581.

Liu, G. R. (2010): *Meshfree Method : Moving Beyond the Finite Element Method,* CRC Press.

Liu, W. K., Jun, S. and Zhang, Y. F. (1995) : Reproduction Kernel Particle methods. *International Journal for Numerical Methods in Fluids,* vol. 20, pp. 1081-1106.

Robert, D. C.; David, S. M.; Michael E. P. (1974): Concepts and applications of finite element analysis, John Wiley & Sons.

Sladek, J.; Stanak, P.; Han, Z-D; Sladek, V.; Atluri, S.N. (2013): Applications of the MLPG Method in Engineering & Sciences: A Review. *Computer Modeling in Engineering & Sciences,* vol. 92, no. 5, pp. 523-475.